Hydrol. Earth Syst. Sci. Discuss., 9, 3657–3690, 2012
www.hydrol-earth-syst-sci-discuss.net/9/3657/2012/
doi:10.5194/hessd-9-3657-2012

Hydrology and Earth System Sciences Discussions

Partitioning of evaporation into transpiration, soil evaporation and interception: a combination of hydrometric measurements and stable isotope analyses

S. J. Sutanto[1,3,*], **J. Wenninger**[1,2], **A. M. J. Coenders-Gerrits**[2], **and S. Uhlenbrook**[1,2]

[1]UNESCO-IHE, Department of Water Engineering, P.O. Box 3015, 2601 DA, Delft, The Netherlands
[2]Delft University of Technology, Water Resources Section, P.O. Box 5048, 2600 GA, Delft, The Netherlands
[3]Research Center for Water Resources, Ministry of Public Works, Jl. Ir. H. Djuanda 193, Bandung 40135, Indonesia
[*]now at: Institute for Marine and Atmospheric Research Utrecht (IMAU), University of Utrecht, Princetonplein 5, 3584 CC, Utrecht, The Netherlands

Received: 8 March 2012 – Accepted: 10 March 2012 – Published: 16 March 2012

Correspondence to: S. J. Sutanto (s.j.sutanto@uu.nl)

Published by Copernicus Publications on behalf of the European Geosciences Union.

HESSD

9, 3657–3690, 2012

Abstract

Best practice agriculture is the key to overcome the food security problem through improvement of water use efficiency. Therefore, knowledge of the water fluxes within the soil-vegetation-atmosphere system is crucial. Many studies have tried to quantify these fluxes, but they encountered difficulties in quantifying the relative contribution of evaporation and transpiration. In this study, we compared four different methods to estimate evaporation fluxes during simulated summer conditions in a grassland lysimeter in the UNESCO-IHE laboratory. Only two of these methods can be used to partition total evaporation into transpiration, soil evaporation and interception. A water balance calculation (whereby rainfall, soil moisture and percolation was measured) and the Penman-Monteith equation were applied to determine total evaporation. A HYDRUS-1D model and isotope measurements were used for the partitioning of total evaporation. The average total evaporation was 3.2 mm d^{-1} calculated with the water balance, 3.4 mm d^{-1} for the Penman-Monteith equation, 3.4 mm d^{-1} calculated with HYDRUS-1D, and 3.1 mm d^{-1} with the isotope mass balance. By use of the isotopes, we separated the total evaporation on average into 2.4 mm d^{-1} transpiration (77.7 %), 0.4 mm d^{-1} soil evaporation (12.2 %), and 0.3 mm d^{-1} interception (10.1 %).

1 Introduction

The Food and Agriculture Organization (FAO) and the United Nations World Food Program (WFP) in Rome stated in September 2010 that 925 million people in the world suffer from chronic hunger. People depend on plants for food and the major environmental factor limiting plant growth is water (Kirkham, 2005). Agriculture needs a huge amount of water and in the future the amount of water needed for irrigation will increase dramatically due to the increasing population. Best practice agriculture is key to overcome this problem through the improvement of water use efficiency. Therefore, knowledge of the water fluxes within the soil-vegetation system and the minimization of

HESSD
9, 3657–3690, 2012

non-productive water fluxes is crucial. Many studies have been carried out to quantify these fluxes by plants, but they encounter difficulties in quantifying the relative contribution of soil evaporation (E_s) and transpiration (E_t) from total evaporation (E) (Shichun et al., 2010).

The use of environmental isotopes (^{18}O and ^{2}H) with their unique attributes present a new and important technique to trace fluxes within soil-plant-atmosphere continuum system (Kendall and McDonnell, 1998; Mook, 2000; Shichun et al., 2010; Wenninger et al., 2010). The reason for using these tracers is that they are chemically and biologically stable and showing no isotopic fractionation during water uptake by roots (Ehleringer and Dawson, 1992; Kendall and McDonnell, 1998; Tang and Feng, 2001; Williams et al., 2004; Balazs et al., 2006; Koeniger et al., 2010). Moreover, partition of the evaporation fluxes using isotopes has been widely proved compared with effective methods such as lysimeter measurements, sapflow measurements, modeling approaches, remote sensing information, and micrometeorological techniques, since these methods have several limitations (Xu et al., 2008; Rothfuss et al., 2010).

An earlier study where evaporation was measured with deuterium had been carried out by Calder et al. (1986) and Calder (1992) in India; however, they only measured the transpiration flux. In the last decade, partitioning of total evaporation into soil evaporation and transpiration using stable isotopes has been studied by Williams et al. (2004); Yepez et al. (2005); Robertson and Gazis (2006); Xu et al. (2008); Rothfuss et al. (2010); Shichun et al. (2010); Wang et al. (2010); Wenninger et al. (2010); Wang et al. (2012). Williams et al. (2004) used the combination of eddy covariance, sapflow, and stable isotopes measurements in an irrigated olive orchard, Morocco. Yepez et al. (2005) estimated the ratio of transpiration from total evaporation using Keeling plots of water vapor under transient conditions. Xu et al. (2008) partitioned soil evaporation and transpiration using a combination of Keeling plots and stable isotopes. Some methods to partition total evaporation are explained by Shichun et al. (2010), such as the mass balance approach, Craig-Gordon formulation, Keeling plot method, and flux-gradient method. Wang et al. (2010) partitioned evaporation based on a combination

HESSD
9, 3657–3690, 2012

of a newly-developed laser-based isotope analyzer and the Keeling plot approach. An isotope mass balance method has been used to partitioning evaporation into soil evaporation and transpiration and is useful to estimate the contribution of evaporation and transpiration during different hydrologic seasons (Ferretti et al., 2003; Robertson and Gazis, 2006; Wenninger et al., 2010). The latest technique to quantify the transpiration flux has been introduced by Wang et al. (2012). They used the mass balance method of both water vapor and water vapor isotopes inside a chamber.

All these studies tried to partition the evaporation fluxes into soil evaporation and transpiration flux only, without taking into account the interception flux. The interception flux in some cases is an important component in the evaporation process and should not be neglected (Savenije, 2004; Gerrits et al., 2009, 2010). Hence, in this study, we report the partitioning of evaporation into soil evaporation and transpiration under consideration of interception using a combination of hydrometric measurements and stable isotopes. Moreover, this method gives more reliable results compared to the other methods and requires only a liquid water isotope analyzer and widely-available hydrometric measurements.

2 Materials and methods

2.1 Experimental set-up

A grassland lysimeter was installed in the laboratory of UNESCO-IHE. The set-up consists of a weighing lysimeter made from a PVC tube with five soil moisture sensors (Decagon 5TE ECH2O probes) and five Rhizon soil moisture samplers (10 cm porous, OD 2.5 mm, sswire, 12 cm tubing) attached to it (Fig. 1). The lysimeter has a length of 40 cm and a diameter of 20 cm and contains soil taken from a grassland area in the Botanical Garden of Delft University of Technology. The soil sample was collected according to the following procedure: (I) the PVC tube was forced into grassland-soil until the PVC tube is completely filled with soil and grass. (II) After filling, the PVC tube

HESSD
9, 3657–3690, 2012

was taken out and sealed at the bottom part. (III) In the laboratory, the PVC tube was installed on top of the percolation device and then was equipped with the soil moisture sensors and Rhizon samplers. (IV) The gap between the PVC tube and percolation device was glued to prevent evaporation from the contact interface of lysimeter and the percolation device.

A wet sieving analysis was carried out to determine the soil types of soil column. The particle distribution used for wet sieving analysis comprises the following: gravel has a diameter more than 2 mm; sand between 63 µm and 2 mm; coarse silt between 38 µm and 63 µm; medium and fine silt and clay less than 38 µm. The results from wet sieving analysis show that the lysimeter contains gravel, sand, silty clay and clay materials. The dominant fractions in the top layer are sand (77 %), clay (16.4 %) and a little gravel and silt. Whereas, the middle layer composes of gravel (25.6 %), sand (47.5 %), clay (22.5 %) and silt (4.3 %), and the bottom layer of sand (62.7 %), clay (27.4 %) and silt and gravel for the rest percentage.

Five soil moisture sensors with an electromagnetic field to measure the dielectric permittivity of the surrounding medium were horizontally pushed into the undisturbed soil to monitor the soil moisture, bulk electrical conductivity (EC), and soil temperature. The probes supply a 70 MHz oscillating wave to the probe prongs that charge the surrounding soil material according to the dielectric permittivity which minimizes salinity and textural effects. The temperature was measured using a surface-mounted thermistor located underneath the probe and will read the temperature of the prong surface. EC was measured by applying an alternating electrical current to two electrodes measuring the resistance between them. The accuracy of 5TE ECH2O probe is 0.08 % for soil moisture, 0.05 dS m^{-1} for EC and 0.1 °C for temperature. The Rhizon soil moisture samplers were installed in the opposite direction of the soil moisture sensors to prevent rapid soil moisture changing due to abstraction of water. The Rhizon samplers are made from a thin hose with a porous filter (0.15–0.2 µm) on top and a connector to attach the syringe in the bottom. The distance interval between two soil moisture sensors as well as the Rhizon samplers was 6.67 cm. The bottom of the lysimeter was filled with

HESSD
9, 3657–3690, 2012

drainage material (diatomaceous earth with diameter of 10 to 200 µm) to enhance the contact between the lysimeter and percolation device.

Percolation was measured using a Decagon drain gauge G2 placed underneath the intact soil monolith. This drain device has a 150 ml reservoir, ±0.1 mm resolution and 10 ms measurement time. The passive-wick system has some limitations, in that there can be a mismatch between the soil water suction and that applied to the wick by the length of the hanging water column (Meissner et al., 2010). However, the differences may be relatively small, especially for sandy soil. Decagon EM50 data loggers with one-minute measurement interval were used to store the data. This set-up was mounted on a Kern DE60K20N platform balance to measure the water losses inside the lysimeter. This device has a maximum weighing range of 60 kg and readability of 20 g. A bucket was placed under the percolation device to store excess water, if the percolated water overflows the percolation device due to the storage limitation. The experiments were carried out from 16 November 2010 until 31 January 2011.

2.2 Sprinkling method

To simulate rainfall, tap water was sprinkled uniformly on the lysimeter with a bucket. The bottom of the bucket perforated many small holes (less than 1 mm diameter) let the water out from the bucket as sprinkled precipitation. The temporal precipitation pattern applied in the laboratory was designed based on the average summer precipitation pattern of a nearby KNMI (Koninklijk Nederlands Meteorologisch Instituut) weather station in Rotterdam for June and July from 2005 to 2010 and it was applied in November and December, 2010, respectively. In January 2011, the precipitation was sprinkled every 3 to 5 days. The accuracy of precipitation sprinkling is around 2 ml. Figure 2 shows the applied precipitation pattern.

HESSD
9, 3657–3690, 2012

2.3 Meteorological measurements

A weather station (Catec Clima Sensor 2000 type 4.9010.00.061) using a Grant Squirrel data logger was installed in the laboratory to measure relative humidity, temperature, wind speed, and solar radiation. The accuracy of the sensors of the weather station is 10 % for the pyranometer, $< 0.5\,m\,s^{-1}$ for wind speed, 0.15 °C for temperature and 3 % for relative humidity. The height difference between measurement devices and lysimeter surface is 15–20 cm.

One lamp (OSRAM powerstar 400 W) was installed above the lysimeter to compensate for the sunlight inside the laboratory. Timers were used to control the lamp and fan. The lamp was switched on at 06:00 a.m. and switched off at 06:00 p.m. The fan was turned on at 06:00 a.m. and turned off at 05:00 p.m. The value range of radiation, wind speed, temperature and humidity is 1–31 $W\,m^{-2}$, 0–1.2 $m\,s^{-1}$, 18–29 °C and 18–45 %, respectively. Evaporation data from the Rotterdam station was used for comparison. Average evaporation calculated with Makkink formula for Rotterdam during summer period (2005 to 2010) is 2.5–3.5 $mm\,d^{-1}$. Daily meteorological measurements in the laboratory are presented in Fig. 3a.

2.4 Isotopes analysis

2.4.1 Isotopes measurements

Soil water was abstracted from every layer in the lysimeter with Rhizon soil moisture samplers by applying a vacuum with 30 ml syringes for the isotope analysis. Water samples were analyzed with the LGR liquid water isotope analyzer (LWIA-24d). The analyzer measures ^{18}O and ^{2}H in liquid water samples with high accuracy (0.2 ‰ and 0.6 ‰, respectively) in a sample volume of < 10 µl. The results are reported in δ values, representing deviations in per-mil (‰) from the Vienna Standard Mean Ocean Water

HESSD
9, 3657–3690, 2012

(VSMOW), defined as

$$\delta = \left(\frac{R_{\text{sample}}}{R_{\text{VSMOV}}} - 1 \right) \cdot 1000 \quad (1)$$

Where R_{sample} is the isotopic abundance ratio of $^2H/H_2O$ in sample and R_{VSMOV} isotopic abundance ratio of the Vienna Standard mean Ocean Water.

2.4.2 Equilibrium and kinetic fractionation

Equilibrium fractionation is the partial separation of isotopes between two or more substances in chemical equilibrium. The fractionation factor is commonly expressed as "$10^3 \ln \alpha$" because this expression is very close to the permil fractionation between the materials and is nearly proportional to the inverse of temperature ($1/T$) at low temperatures in Kelvin (Kendall and McDonnell, 1998). Szapiro and Steckel (1967) and Majoube (1971) as cited in Clark and Fritz (1997) give the following equation to quantify the equilibrium fractionation factor from liquid (A) to vapor phase (B).

$$10^3 \ln \alpha_{\text{A-B}} = \frac{10^6 a}{T^2} + \frac{10^3 b}{T} + c \quad (2)$$

T is temperature in Kelvin, constants a, b and c for ^{18}O are $a = 1.137$, $b = -0.4156$, and $c = -2.0667$ and $a = 24.844$, $b = -76.248$ and $c = 52.612$ for ^2H.

The other fractionation process is the kinetic fractionation which is a process that separates stable isotopes from each other by their mass during un-idirectional processes. The factors that affect kinetic fractionation of water during the evaporation process are humidity, salinity and temperature. The effect of humidity on isotope enrichment can be expressed as follows (h is humidity, %):

$$10^3 \ln \alpha^{18}O_{\text{A-B}} = 14.2\,(1-h)\,‰ \quad (3)$$

$$10^3 \ln \alpha^{2}H_{\text{A-B}} = 12.5\,(1-h)\,‰ \quad (4)$$

HESSD
9, 3657–3690, 2012

2.5 Evaporation analysis

Evaporation in this study was calculated using a water balance, the Penman-Monteith equation, HYDRUS-1D numerical model, and isotopes mass balance. The water balance, HYDRUS-1D model, and isotopes mass balance calculate the actual evaporation, while the Penman-Monteith equation calculates the potential evaporation.

2.5.1 Water balance

With this method, evaporation is calculated based on the differences between precipitation, storage changes, and percolation. The weighing balance measures the storage changes in the lysimeter directly. The water balance formula is described as a follows:

$$E = P - P_e - \frac{dS}{dt} \quad (5)$$

Where P is precipitation ($L T^{-1}$), E evaporation ($L T^{-1}$), P_e percolation ($L T^{-1}$), and dS/dt changes of storage in the soil ($L T^{-1}$).

2.5.2 Penman-Monteith

Penman-Monteith is the most physically-based method to calculate potential evaporation compared with the other equations such as Makkink, Thornthwaite or Blaney Criddle, since this method considers the aerodynamic resistance and crop resistance beside some meteorological parameters. The aerodynamic resistance is calculated with a measuring height of 20 cm. The Penman-Monteith formula is defined in Eq. (6). Detailed information on the Penman-Monteith method can be found at Howell and Evett (2004) and Allen et al. (1998).

$$E_p = \frac{C}{L}\left(\frac{sR_N + c_p\rho_a(e_s - e_d)/r_a}{s + \gamma(1 + r_c/r_a)}\right) \quad (6)$$

HESSD
9, 3657–3690, 2012

Where E_p is the potential evaporation of grass ($L T^{-1}$), ρ the density of water ($M L^{-3}$), R_N net radiation at the earth's surface ($M T^{-3}$), L latent heat of vaporization ($L = 2.45 \times 10^6 J kg^{-1}$), s the slope of the temperature-saturation vapor pressure curve ($M T^{-2} L^{-1} K^{-1}$), c_p the specific heat of air at constant pressure ($c_p = 1004.6 J kg^{-1} K^{-1}$), ρ_a the density of air ($M L^{-3}$) ($1.2047 kg m^{-3}$ at sea level), e_d actual or dew point vapor pressure of the air at 2 m height (kPa), e_s saturation vapor pressure for the air temperature at 2 m height ($M T^{-2} L^{-1}$), γ psychometric constant ($M T^{-2} L^{-1} K^{-1}$) ($\gamma = 0.067 kPa K^{-1}$ at sea level), r_a the aerodynamic resistance ($T L^{-1}$), and r_c the crop resistance ($T L^{-1}$) ($r_c = 70 s m^{-1}$ for grass, Allen et al., 1998).

Since the water balance method estimates actual evaporation and Penman-Monteith the potential evaporation, evaporation estimates of the water balance should theoretically not exceed the results from Penman-Monteith. Thus, if the Penman-Monteith equation will be used to calculate actual evaporation, the results from Penman-Monteith need to be reduced using a reduction factor (e.g., Sumner and Jacobs, 2005).

2.5.3 HYDRUS-1D model

The HYDRUS-1D model can be used to simulate the water and solute movement in unsaturated, partly saturated or fully saturated porous media (Simunek et al., 2008). The HYDRUS-1D model for one-dimensional water movement is based on the modified Richards equation with the assumption that the air phase plays an unimportant role in the liquid flow process and water flow due to neglect of thermal gradient. In this study, the HYDRUS-1D modeling has been divided into three parts. The first part is the calibration process to obtain the soil parameters. By inverse modeling the model was calibrated on the observed soil moisture data. The second part is the validation process and the last part is the complete simulation from November to January. Calibration and validation were carried out from the first to the end of December and the first of January to the end of January, respectively.

HESSD
9, 3657–3690, 2012

We schematized our soil column as two soil layers. The top layer (0–6.67 cm) consists of sand whereas the bottom layer (33.3–40 cm) of clay-silt. We used the default soil parameters from the HYDRUS-1D soil database as starting parameter. Root depth was observed at 5 cm. Hence in the model, we used the root distribution value of one for the surface which decreased to zero in the depth more than 5 cm. Initial soil moisture was obtained from the soil moisture sensors which was 0.22 ($m^3\,m^{-3}$) for the surface layer to 0.38 ($m^3\,m^{-3}$) at the bottom. The Feddes root water uptake model was chosen to simulate the amount of water taken up from the soil for transpiration using the default parameters for grass (Feddes et al., 1974, 2001). Inverse modeling was performed to estimate the calibrated parameters. In this model, soil hydraulic properties are assumed to be described by an analytical model. The soil parameters are optimized. The HYDRUS-1D model uses a R^2 value for goodness of fit test. The time step used in this model is hourly with length unit in mm. The single porosity Van Genuchten-Mualem model was used for the soil hydraulic model simulation without hysteresis. The boundary conditions used in this model are the atmospheric boundary condition for the upper boundary and free drainage for the bottom boundary. See Simunek et al. (2008) for more detailed information regarding the HYDRUS-1D theory, method and default parameters.

2.5.4 Isotope mass balance calculation

The isotope mass balance calculation has been carried out to calculate the amount of water used for soil evaporation and transpiration. The assumption used in this calculation is that the water taken by plant roots for transpiration is not affected by isotope fractionation until the water is leaving the plant via the stomata (Ehleringer and Dawson, 1992; Kendall and McDonnell, 1998; Tang and Feng, 2001; Riley et al., 2002; Williams et al., 2004; Balazs et al., 2006; Gat, 2010). In contrast, the evaporated water from the soil and interception are affected by isotope fractionation. Therefore, interception needs to be subtracted from the precipitation in order to get the net precipitation, which is assumed to have the same isotopic concentration as the precipitation. The net

HESSD
9, 3657–3690, 2012

precipitation is not mixed with the (partly) fractionated interception water on the grass. Hence, in the isotope mass balance calculation we used the net precipitation values. Section 2.6 is explained how interception is estimated. The isotopes mass balance can be formulated as:

$$m_i + m_p = m_v + m_f + m_t + m_z = m_{total} \quad (7)$$

and

$$\delta_i x_i + \delta_p x_p = \delta_v x_v + \delta_f x_f + \delta_t x_t + \delta_z x_z \quad (8)$$

Where m_i (M) is the initial mass, m_p (M) net precipitation mass, m_v (M) evaporation mass, m_f (M) final mass, m_t (M) transpiration mass, m_z (M) percolation mass. δ represents e.g. the $\delta^{18}O$ (permil) of each component and x the fraction of water in respective component. Thus, δ_i is $\delta^{18}O$ for the initial measurement, δ_p is $\delta^{18}O$ for the net precipitation, δ_v is $\delta^{18}O$ for evaporation, δ_f is $\delta^{18}O$ for final measurement, δ_t is $\delta^{18}O$ for transpiration, δ_z is $\delta^{18}O$ for percolation. m_{total} is calculated from the initial soil water mass and precipitation mass ($m_{total} = m_i + m_p$) and the fraction of each component is calculated as $x_j = m_j/m_{total}$.

The isotopic content of transpired water and deep percolated water are not affected by isotopic fractionation and we can combine these terms as non fractionation terms (x_{nf}). Moreover, the isotopic content of this water is equal to the average δ value of soil water over time interval δ_i and δ_f (Robertson and Gazis, 2006).

$$x_{nf} = x_t + x_z \quad (9)$$

$$\delta_{nf} = \delta_t = \delta_z \quad (10)$$

$$\delta_t = \delta_z = \frac{(\delta_i + \delta_f)}{2} \quad (11)$$

The unknown fraction of evaporated water (x_v) and transpired water (x_t) can be calculated using Eq. (5) if the isotopic values of transpiration water (δ_t) is assumed as

HESSD
9, 3657–3690, 2012

a mixture of initial soil water (δ_i) and final soil water (δ_f). The δ value of evaporated water was calculated using equilibrium and kinetic fractionation. Thus, Eq. (2) can be derived into Eq. (6) and then substitute it with Eqs. (3–5) to solve x_t and x_v as unknown variables (Eq. 7):

$$x_v = \frac{x_i\delta_i + x_p\delta_p - x_f\delta_f - (x_t + x_z)\delta_z}{\delta_v} \quad (12)$$

$$x_v = \frac{x_i\delta_i + x_p\delta_p - x_f\delta_f - x_p\delta_{nf} + x_f\delta_{nf} - x_i\delta_{nf}}{\delta_v - \delta_{nf}} \quad (13)$$

and

$$x_{nf} = x_p + x_i - x_v - x_f \quad (14)$$

2.6 Interception

Interception is the part of rainfall that is intercepted by the earth's surface such as vegetation, soil surface, litter, rock, roads, etc (Sutanudjaja et al., 2011; Gerrits, 2010; Savenije, 2004). Interception can be defined as a stock, flux or the entire interception process (Gerrits et al., 2007, 2010). The stock refers to the amount of water that grass can store (i.e. the storage capacity), and flux refers to successive evaporation from this storage. Gerrits (2010) measured for a grassland area in Westerbork (the Netherlands) a storage capacity of 2 mm. Both the isotope mass balance calculation and the HYDRUS-1D model use the interception flux, thus the stock values (mm) need to be converted into flux values (mm day^{-1}) by multiplying the stock value with the mean number of precipitation events per day to get the daily interception threshold (Gerrits et al., 2009). In this case we have 30 rainfall events in 77 days. This results in a daily interception threshold, D of 1 mm day^{-1}. For the HYDRUS-1D model we calibrated the parameters "a" of the interception module in such way that D equals 1 mm day^{-1} (see Eq. 15). For the isotope mass balance calculation we applied Eq. (16). The interception

HESSD
9, 3657–3690, 2012

formula from the HYDRUS model and the net precipitation are described as follows:

$$D = a \cdot \mathrm{LAI}\left(1 - \frac{1}{1 + \frac{bP}{a \cdot \mathrm{LAI}}}\right) \quad (15)$$

$$\mathrm{LAI} = 0.24 \cdot h_{\mathrm{grass}} \quad (16)$$

$$b = \mathrm{SCF} = 1 - \exp(-a_i \cdot \mathrm{LAI}) \quad (17)$$

$$P_{\mathrm{net}} = \max(P - D, 0) \quad (18)$$

where D is the daily interception threshold ($\mathrm{L\,T^{-1}}$), h_{grass} the grass height, a_i r_{Extinct} = 0.463, LAI the leaf area index ($\mathrm{L\,L^{-1}}$), P precipitation ($\mathrm{L\,T^{-1}}$), and a the constant entered from the HYDRUS-1D interface (we got 4.5 mm).

3 Results and discussion

3.1 Soil water content and HYDRUS-1D modeling

The results from the climate station and soil water content measurements are illustrated in Fig. 3. The fluctuation of soil moisture is strongly influenced by rainfall. The range in soil moisture is between 0.22 and 0.47 ($\mathrm{m^3\,m^{-3}}$). The sensors in the upper part are mostly affected by precipitation. Depth of 6.7 and 13.3 cm from top showed indeed a quick response to precipitation, but depth of 26.6 cm from top showed also a quick response. In contrast, depth of 33.3 cm from top as the bottom part showed a less response to the precipitation water. The fast response at depth 13.3 and 26.6 cm can be caused by macropores in the soil, soil cracking, or flow at the boundary between the soil and PVC pipe.

The HYDRUS-1D model was used to simulate the water fluxes inside the lysimeter. The calibration results for both materials is good with R^2 = 0.94. Table 1 showed the calibrated parameters. After calibration, the calibrated parameters were used to simulate the data in January to validate the model. The validation results are acceptable

HESSD
9, 3657–3690, 2012

although the R^2 value is 0.82. The calibration and validation results starting from December to January are presented in Fig. 4 and the calibrated parameters in Table 1, where Θ_r presents the residual water content, Θ_s saturated water content, α and n parameters describing the shape of soil water retention curve and hydraulic conductivity curve, K_s is the saturated hydraulic conductivity and l the pore-conductivity.

Figure 4 shows that the simulation results for material 1 are unable to capture some peak values although the recession limbs from the model fit the observation. However, material 2 shows that the observed values and simulated values agree well. In addition, percolation can also be used for model calibration. Total modeled percolation in December 2010 is 0.1 mm month^{-1} while the observed percolation 0.4 mm month^{-1}. However, total percolation during the entire measurement period (3 months) is 2.4 mm and total percolation simulated by the HYDRUS-1D model 0.35 mm (Fig. 5).

Although the total observed percolation is 2.4 mm and total observed is 0.35 mm, the percolation result from the model is still acceptable. The percolation error is 2.05 mm in three months or less than 1 mm per month. The difference between model results and observations might be caused by macro-pores, roots, soil cracking, etc. HYDRUS-1D assumes a perfect homogenous soil column while, in fact, the soil column may contain those causative factors.

3.2 Isotope composition of soil water

The isotope composition of soil water is shown in Fig. 6. As expected, the isotope results show that the water inside the lysimeter is affected by evaporation in non-equilibrium processes which is indicated by a slope less than 8 for evaporation (Dansgaard, 1964). The overall evaporation line has a slope of 3.6 and an intercept value of −19.7 ‰ (R^2 = 0.99). The soil water at depth (z) 6.6 cm has an evaporation slope of 3.9 and an intercept value of −19.6 ‰, for z = 13.3 cm, the line has a slope of 3.8 and an intercept of −20.2 ‰, and for z = 20 cm, an evaporation slope of 3.6 and an intercept value of −19.7 ‰. These slope values are comparable with other studies in

HESSD
9, 3657–3690, 2012

vadose zones which have evaporation slopes between 2 to 5 (Allison, 1982; Clark and Fritz, 1997; Kendall and McDonnell, 1998; Wenninger et al., 2010). The evaporation line shows that kinetic enrichment of ^{18}O in evaporating water is more than ^{2}H. The water in the upper part of the lysimeter has as expected higher soil evaporation rates compared to the water in the lower part of the soil. Precipitation, soil moisture at z = 33.3 cm, and some of the samples at z = 26.6 cm are laying on the GMWL. This means that evaporation has little effect on the bottom part of the lysimeter.

For a better overview of the isotope fractionation, the isotope values are plotted against depth and time (see Fig. 7a). High values of ^{2}H and ^{18}O appear at depths of 6.6, 13.3, and 20 cm and the highest value occurs at a depth of 20 cm from the soil surface. It shows that the effect of evaporation occurs from the surface until 20 cm depth and the maximum value at 20 cm depth is called the drying front. This process is caused by kinetic effects of diffusion (Kendall and McDonnell, 1998; Clark and Fritz, 1997). The shape of this profile is performed by isotope vapor diffusion. The shape from the surface to 20 cm depth is performed by vapor diffusion and the shape from below 20 cm depth is caused by downward diffusion of isotopes. Rain water originated from tap water shows an isotope composition of −40 to −50 ‰ for ^{2}H. Percolation water has an isotope range between −15 to −30 ‰ and is more enriched compared to the isotope value from depth 33.3 cm. This enrichment of isotopes in the percolation water might be caused by the evaporation process inside the percolation meter and mixing water from the top layer which is isotopically enrich. The percolation meter is not a completely closed device and there might be a crack inside the lysimeter between soil column and PVC.

To analyze the relationship between storm size and enrichment, we plotted per rain event the $\Delta^{18}O$ (see Fig. 7b). $\Delta^{18}O$ is the differences between $\delta^{18}O$ from the next sampling ($\delta^{18}O_{t+1}$) minus $\delta^{18}O$ before the rain event ($\delta^{18}O_t$). Figure 6b shows that small precipitation events have more enrichment of $\delta^{18}O$. On the contrary, heavy storm events hardly enrich in their isotopic composition in one day. Storm sizes of 3.2 mm, 6.4 mm, 9.5 mm and 21.6 mm have a maximum $\Delta^{18}O$ in fractionation of 11.2 ‰, 9.9 ‰,

HESSD
9, 3657–3690, 2012

8.9 ‰ and 0.5 ‰, respectively. The bigger the storm event, the smaller the enrichment. In contrast, the smaller the storm, the bigger the enrichment. This phenomenon may be explained by the mobile and immobile soil water concept. Soil water inside small pores (e.g. clay less than 2 µm diameter) is immobile compared with soil water in large pores (e.g. sand more than 0.3 mm diameter) which is mobile. These small pores have a long water-residence time and can only be replaced with heavy precipitation events (Brooks et al., 2010). Therefore, heavy storms replenish all water inside the soil pores both mobile and immobile. Thus, the isotope composition in the soil water is hardly becoming enriched. However, small storms only replace the mobile soil water and the Rhizon sampler abstracts the mixing water between mobile and immobile water (which may have a heavily isotope composition due to evaporation) after several days.

3.3 Evaporation analysis

The evaporation analysis has been carried out using the Penman-Monteith equation, the water balance, the HYDRUS-1D model, and the isotopes mass balance for comparison. In Fig. 8 the results for the four methods are compared. Actual evaporation calculated with the water balance method is believed to be the most accurate actual evaporation calculation compared to the other methods, since this method uses a weighing balance to measure the losses of water inside the lysimeter directly due to evaporation and percolation. The evaporation estimation of the isotope mass balance, the HYDRUS-1D model and water balance calculation is in good agreement, while the Penman-Monteith estimation is higher. This is logic because Penman-Monteith estimates the potential evaporation. Total evaporation during the simulation period of 77 days was 237.3 mm calculated with the isotope mass balance, 243.1 mm calculated with the water balance, 260.1 mm calculated with HYDRUS-1D, and 265.6 mm calculated with Penman-Monteith. From the differences between actual evaporation and potential evaporation during measurements, it is shown that there was water shortage of 28.3 mm, 22.6 mm and 5.5 mm calculated with isotope mass balance, water balance, and HYDRUS-1D, respectively. Average total evaporation was 3.1 mm d^{-1},

HESSD
9, 3657–3690, 2012

3.2 mm d^{-1}, 3.4 mm d^{-1} and 3.4 mm d^{-1} calculated with isotope mass balance, water balance, Penman-Monteith and HYDRUS-1D.

Average evaporation (3.1 mm d^{-1}) can be partitioned into 0.4 mm d^{-1} for soil evaporation, 0.3 mm d^{-1} for interception and 2.4 mm d^{-1} for transpiration using the isotope mass balance. Hence, the proportion of soil evaporation is 12.2 %, interception 10.1 % and transpiration 77.7 % (Table 1 summarizes the results). Interception evaporation and soil evaporation contribute almost equal to the total actual evaporation, this shows that the interception process plays a significant role.

Some studies (e.g., Herbst et al., 1996; Ferretti et al., 2003; Robertson and Gazis, 2006; Roupsard et al., 2006; Xu et al., 2008; Wang et al., 2010; Wenninger et al., 2010) including the FAO crop model calculated that the percentage of transpiration is more or less 70%. The results from the HYDRUS-1 D model also show that 26.9 % of total evaporation is evaporated from the soil, 64.1 % transpired and 8.9 % intercepted. The HYDRUS-1D model calculated the transpiration flux based on water uptake distribution (Feddes et al., 1978; Genuchten, 1987; Simunek et al., 2008).

4 Conclusions

To improve water use efficiency in agriculture, knowledge about water fluxes in the vadose zone is essential. The combination of hydrometric measurements and stable isotopes can accurately estimate these water fluxes. Hydrometric measurements can provide the information of water in, out and storage changes inside the lysimeter. Futhermore, isotopes can be used to partition the evaporation fluxes.

Measurements of stable isotopes show a great prospective to partition the evaporation fluxes by using the isotopes mass balance calculation. Total evaporation calculated with isotopes is comparable to the results from the water balance method and HYDRUS-1D. However, the isotope measurements have the advantage that they enable to partition the evaporation flux into the productive (transpiration) and non-productive fluxes (soil evaporation and interception). Our findings show that the

HESSD
9, 3657–3690, 2012

interception flux is a significant process since the interception flux may have the same value as the soil evaporation flux. However, most of the evaporation is coming from transpiration. During the experiment, transpiration indicated 2.4 mm d^{-1}, soil evaporation 0.4 mm d^{-1}, and interception 0.3 mm d^{-1} calculated using isotope mass balance. This resulted in a E_t/E ratio of 0.76.

Acknowledgements. This study was carried out as a joint research between UNESCO-IHE, Delft, the Netherlands and IAEA isotope hydrology section, Vienna, Austria and financed by the Coordinated Research Project No 1429 (CRP 1429). The authors would also like to thank the UNESCO-IHE laboratory staff for their great support.

References

Allen, R. G., Pereira, L. S., Raes, D., and Smith, M.: Crop evapotranspiration-guidlines for computing crop water requirements-FAO irrigation and drainage paper 56, FAO-Food and Agriculture Organization of the United Nations, ISBN 92-5-104219-5, 1998. 3666, 3667

Allison, G. B.: The relationship between ^{18}O and deuterium in water in sand columns undergoing evaporation, J. Hydrol., 55, 163–169, 1982. 3673

Balazs, M. F., John, G. B., Pradeep, A., and Charles, J. V.: Application of isotope tracers in continental scale hydrological modeling, J. Hydrol., 330, 444–456, doi:10.1016/j.jhydrol.2006.04.029, 2006. 3660, 3668

Brooks, J. R., Barnard, H. R., Coulombe, R., and McDonnell, J. J.: Ecohydrologic separation of water between trees and streams in a mediterranean climate, Nat. Geosci., 3, 100–104, 2010. 3674

Calder, I. R.: Deuterium tracing for the estimation of transpiration from trees Part 2. Estimation of transpiration rates and transpiration parameters using a time-averaged deuterium tracing method, J. Hydrol., 130, 27–35, 1992. 3660

Calder, I. R., Narayanswamy, M. N., Srinivasalu, N. V., Darling, W. G., and Lardner, A. J.: Investigation into the use of deuterium as a tracer for measuring transpiration from eucalypts, J. Hydrol., 84, 345–351, 1986. 3660

Clark, I. and Fritz, P.: Environmental Isotopes in Hydrogeology, CRC Press, Boca Raton, FL, 1997. 3665, 3673

HESSD

9, 3657–3690, 2012

Dansgaard, W.: Stable isotopes in precipitation, Tellus, 16, 436–468, 1964.
Ehleringer, J. R. and Dawson, T. E.: Water uptake by plants: perspectives from stable isotope composition, Plant Cell Environ., 15, 1073–1082, 1992. 3660, 3668
Feddes, R. A., Bresler, E., and Neuman, S. P.: Field test of a modified numerical model for water uptake by root systems, Water Resour. Res., 10, 1199–1206, 1974. 3668
Feddes, R. A., Kowalik, P. J., and Zaradny, H.: Simulation of Field Water Use and Crop Yield, John Wiley & Sons, New York, NY, 1978. 3675
Feddes, R. A., Hoff, H., Bruen, M., Dawson, T., de Rosnay, P., Dirmeyer, P., Jackson, R. B., Kabat, P., Kleidon, A., Lilly, A., and Pitman, A.: Modeling root water uptake in hydrological and climate models, B. Amer. Meteorol. Soc., 82, 2797–2809, 2001. 3668
Ferretti, D. F., Pendall, E., Morgan, J. A., Nelson, J. A., LeCain, D., and Mosier, A. R.: Partitioning evapotranspiration fluxes from a Colorado grassland using stable isotopes: seasonal variations and ecosystem implications of elevated atmospheric CO_2, Plant Soil, 254, 291–303, 2003. 3661, 3675
Gat, J. R.: Isotope Hydrology a Study of the Water Cycle, Imperial College Press, London, 2010. 3668
Gehrels, J. C., Peeters, J. E. M., Vries, J. J., and Dekkers, M.: The mechanism of soil water movement as inferred from ^{18}O stable isotope studies, Hydrol. Sci. J., 43, 579–594, 1998.
van Genuchten, M. T.: A numerical model for water and solute movement in and below the root zone. Research Report No 121, US Salinity Laboratory, USDA, ARS, Riverside, California, 1987. 3675
Gerrits, A. M. J.: The role of interception in the hydrological cycle, PhD thesis, Delft University of Technology, The Netherlands, 2010. 3670
Gerrits, A. M. J., Savenije, H. H. G., Hoffmann, L., and Pfister, L.: New technique to measure forest floor interception – an application in a beech forest in Luxembourg, Hydrol. Earth Syst. Sci., 11, 695–701, doi:10.5194/hess-11-695-2007, 2007. 3670
Gerrits, A. M. J., Savenije, H. H. G., Veling, E. J. M., and Pfister, L.: Analytical derivation of the Budyko curve based on rainfall characteristics and a simple evaporation model, Water Resourc. Res., 45, W04403, doi:10.1029/2002GB001878, 2009. 3661, 3670
Gerrits, A. M. J., Pfister, L., and Savenije, H. H. G.: Spatial and temporal variability of canopy and forest floor interception in a beech forest, Hydrol. Process. 24, 3011–3025, doi:10.1002/hyp.7712, 2010. 3661, 3670

HESSD
9, 3657–3690, 2012

Herbst, M., Kappen, L., Thamm, F., and Vanselow, R.: Simultaneous measurements of transpiration, soil evaporation and total evaporation in a maize field in Northern Germany, J. Exp. Bot., 47, 305, 1957–1962, 1996. 3675

Howell, T. A. and Evett, S. R.: The Penman-Monteith method. Section 3 in Evapotranspiration: Determination of Consumptive Use in Water Rights Proceedings, Continuing Legal Education in Colorado, Inc. Denver, CO, 2004. 3666

Kendall, C. and McDonnell, J. J.: Isotope Tracers in Catchment Hydrology, Elsevier, Amsterdam, 1998. 3660, 3665, 3668, 3673

Kirkham, M. B.: Principles of Soil and Plant Water Relations, Elsevier, USA, 2005. 3659

Koeniger, P., Leibundgut, C., Link, T., and Marshall, J. D.: Stable isotopes applied as water traces in column and field studies, Org. Geochem., 41, 31–40, doi:10.1016/j.orggeochem.2009.07.006, 2010. 3660

Meissner, R., Rupp, H., Seeger, J., Ollesch, G., and Gee, G. W.: A comparison of water flux measurements: passive wick-samplers versus drainage lysimeters, Soil Sci., 61, 609–621, doi:10.1111/j.1365-2389.2010.01255.x, 2010. 3663

Mook, W. G.: Environmental Isotopes in the Hydrological Cycle – Principles and Applications, UNESCO-IHP, Paris, 2000. 3660

Riley, W. J., Still, C. J., Torn, M. S., and Berry, J. A.: A mechanistic model of $H_2{}^{18}O$ and $C^{18}OO$ fluxes between ecosystems and the atmosphere: model description and sensitivity analyses, Global Biogeochem. Cy., 16, 42.41–42.14, doi:10.1029/2002GB001878, 2002. 3668

Robertson, J. A. and Gazis, C. A.: An oxygen isotope study of seasonal trends in soil water fluxes at two sites along a climate gradient in Washington state (USA), J. Hydrol., 328, 375–387, doi:10.1016/j.jhydrol.2005.12.031, 2006. 3660, 3661, 3669, 3675

Rothfuss, Y., Biron, P., Braud, I., Canale, L., Durant, J.-L., Gaudet, J.-P., Richard, P., Vauclin, M., and Bariac, T.: Partitioning evapotranspiration fluxes into soil evaporation and plant transpiration using water stable isotopes under controlled conditions, Hydrol. Process, 3177–3194, doi:10.1002/hyp.7743, 2010. 3660

Roupsard, O., Bonnefond, J.-M., Irvine, M., Berbigier, P., Nouvellon, Y., Dauzat, J., Taga, S., Hamel, O., Jourdan, C., Saint-Andre, L., Mialet-Serra, I., Labouisse, J.-P., Epron, D., Joffre, R., Braconnier, S., Rouziere, A., Navarro, M., and Bouillet, J.-P.: Partitioning energy and evapo-transpiration above and below a tropical palm canopy, Agr. Forest Meteorol., 139, 252–268, doi:10.1016/j.agrformet.2006.07.006, 2006. 3675

HESSD

9, 3657–3690, 2012

Savenije, H. H. G.: The importance of interception and why we should delete the term evapotranspiration from our vocabulary, Hydrol. Process., 18, 1507–1511, doi:10.1002/hyp.5563, 2004. 3661, 3670

Shichun, Z., Xuefa, W., Jianlin, W., Guirui, Y., and Xiaomin, S.: The use of stable isotopes to partition evapotranspiration fluxes into evaporation and transpiration, Acta Ecol. Sin. Elsevier, 30, 201–209, doi:10.1016/j.chnaes.2010.06.003, 2010. 3660

Simunek, J., Sejna, M., Saito, H., Sakai, M., and van Genuchten, M. T.: The HYDRUS 1D software package for simulating the one-dimensional movement of water, heat, and multiple solutes in variability-saturated media, University of California Riverside, California, 281 pp., 2008. 3667, 3668, 3675

Sumner, D. M. and Jacobs, J. M.: Utility of Penman-Monteith, Priestley-Taylor, reference evapotranspiration, and pan evaporation methods to estimate pasture evapotranspiration, J. Hydrol., 308, 81–104, doi:10.1016/j.jhydrol.2004.10.023, 2005. 3667

Sutanudjaja, E. H., van Beek, L. P. H., de Jong, S. M., van Geer, F. C., and Bierkens, M. F. P.: Large-scale groundwater modeling using global datasets: a test case for the Rhine-Meuse basin, Hydrol. Earth Syst. Sci., 15, 2913–2935, doi:10.5194/hess-15-2913-2011, 2011. 3670

Tang, K. and Feng, X.: The effect of soil hydrology on the oxygen and hydrogen isotopic compositions of plants source water, Earth Planet. Sci. Lett., 185, 355–367, 2001. 3660, 3668

Wang, L., Caylor, K. K., Villegas, J. C., Barron-Gafford, G. A., Breshears, D. D., and Huxman, T. E.: Partitioning evapotranspiration across gradients of woody plant cover: assessment of a stable isotope technique, Geophys. Res. Lett., 37, L09401, doi:10.1029/2010GL043228, 2010. 3660, 3675

Wang, L., Good, S. P., Caylor, K. K., and Cernusak, L. A.: Direct quantification of leaf transpiration isotopic composition, Agric. Forest Meteorol., 154–155, 127–135, doi:10.1016/j.agrformet.2011.10.018, 2012. 3660, 3661

Wenninger, J., Beza, D. T., and Uhlenbrook, S.: Experimental investigations of water fluxes within the soil-vegetation-atmosphere system: stable isotope mass-balance approach to partition evaporation and transpiration, Phys. Chem. Earth, 35, 565–570, doi:10.1016/j.pce.2010.07.016, 2010. 3660, 3661, 3673, 3675

Williams, D. G., Cable, W., Hultine, K., Hoedjes, J. C. B., Yepez, E. A., Simonneaux, V., Erraki, S., Boulet, G., de Bruin, H. A. R., Chehbouni, A., Hartogensis, O. K., and Timouk, F.: Evapotranspiration components determined by stable isotope, sap flow and eddy covariance

HESSD

9, 3657–3690, 2012

techniques, Agric. Forest Meteorol., 125, 241–258, doi:10.1016/j.agrformet.2004.04.008, 2004. 3660, 3668

Xu, Z., Yang, H., Liu, F., An, S., Cui, J., Wang, Z., and Liu, S.: Partitioning evapotranspiration flux components in a subalpine shrubland based on stable isotopic measurements, Bot. Stud., 49, 351–361, 2008. 3660, 3675

Yepez, E. A., Huxman, T. E., Ignace, D. D., English, N. B., Weltzin, J. F., Castellanos, A. E., and Williams, D. G.: Dynamics of transpiration and evaporation following a moisture pulse in semiarid grassland: A chamber-based isotopes method for partitionong flux components, Agric. Forest Meteorol., 132, 359–276, doi:10.1016/j.agrformet.2005.09.006, 2005. 3660

HESSD

9, 3657–3690, 2012

Table 1. The calibrated parameters from HYDRUS-1D inverse modeling (Θ_r is the residual water content, Θ_s saturated water content, α and n parameters describing the shape of soil water retention curve and hydraulic conductivity curve, K_s saturated hydraulic conductivity and l pore-conductivity).

Name	Θ_r ($cm^3\,cm^{-3}$)	Θ_s ($cm^3\,cm^{-3}$)	α (cm^{-1})	n (–)	K_s ($cm\,day^{-1}$)	l ($cm\,cm^{-1}$)
Material 1	0.12960	0.50069	0.00152	1.76900	4.53730	0.34815
Material 2	0.17852	0.39118	0.00077	1.05420	0.32555	0.55768

HESSD
9, 3657–3690, 2012

Table 2. Evaporation analysis summary from 16 of November 2010 until 27 of January 2011. E is total evaporation, E_s soil evaporation, E_t transpiration and E_i interception, while $\overline{E}$ is the mean total evaporation, $\overline{E}_s$ mean soil evaporation, $\overline{E}_t$ mean transpiration and $\overline{E}_i$ mean interception.

Methods	E (mm)	E_s (mm)	E_t (mm)	E_i (mm)	$\overline{E}$ (mm day^{-1})	$\overline{E}_s$ (mm day^{-1})	$\overline{E}_t$ (mm day^{-1})	$\overline{E}_i$ (mm day^{-1})
Penman-Monteith	265.6	–	–	–	3.4	–	–	–
Water balance	243.1	–	–	–	3.2	–	–	–
HYDRUS-1D	260.1	70.2	166.6	23.3	3.4	0.9 (26.9 %)	2.2 (64.1 %)	0.3 (8.9 %)
Isotope mass balance	237.3	28.8	184.5	24	3.1	0.4 (12.2 %)	2.4 (77.7 %)	0.3 (10.1 %)

HESSD
9, 3657–3690, 2012

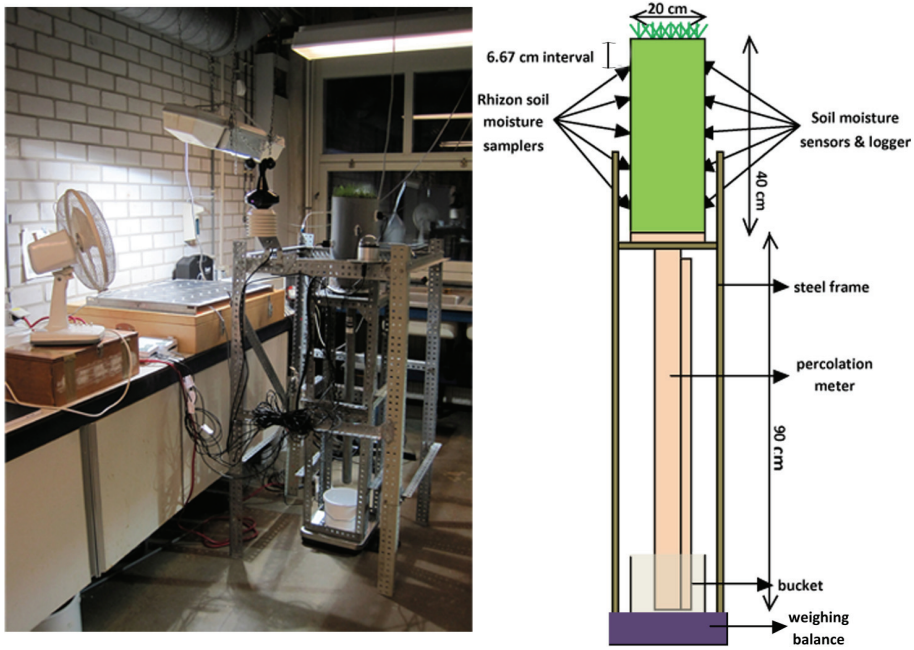

Fig. 1. Photo and schematic sketch of the experimental set-up.

HESSD
9, 3657–3690, 2012

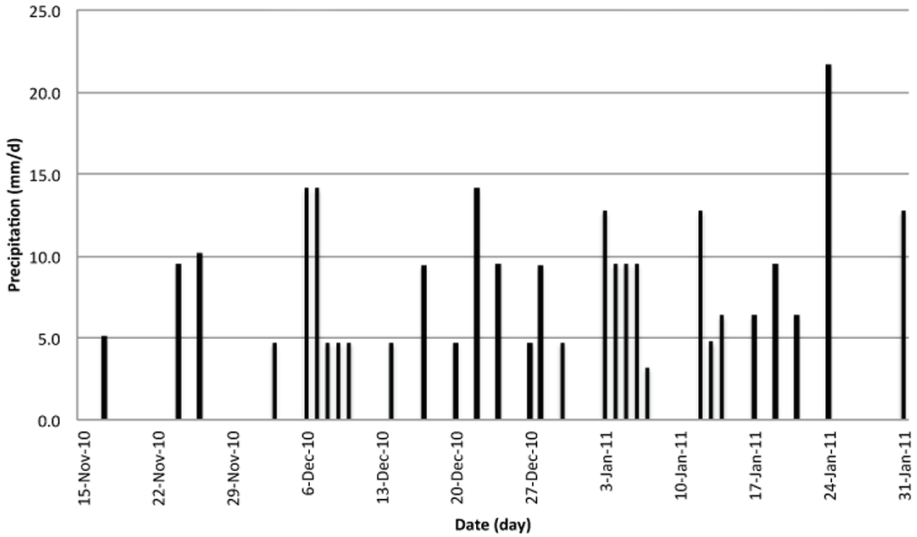

Fig. 2. The applied precipitation in UNESCO-IHE laboratory.

HESSD
9, 3657–3690, 2012

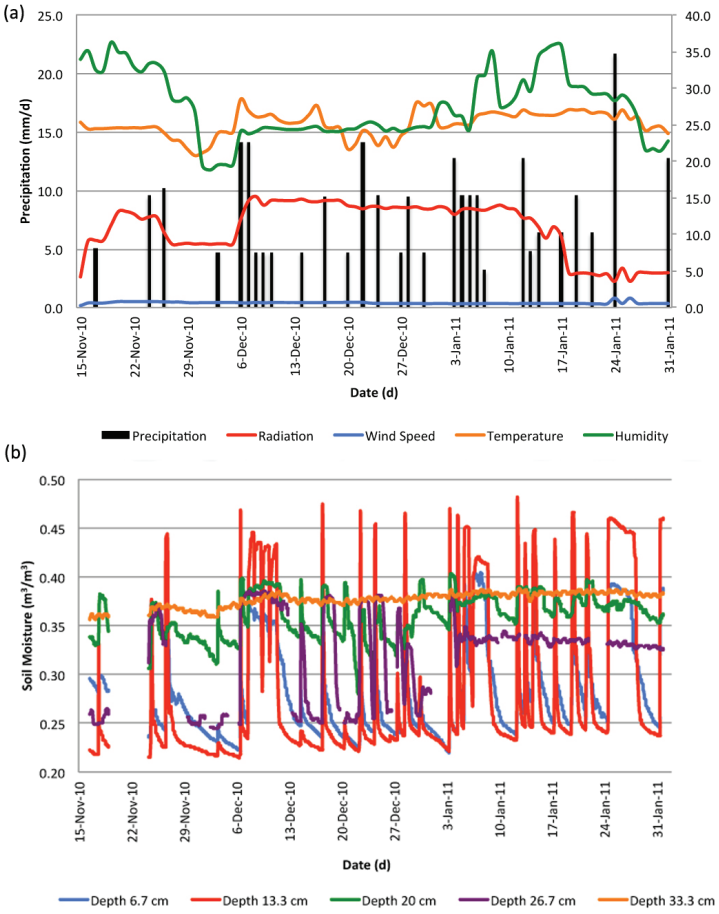

Fig. 3. Climatologic data measured at the UNESCO-IHE laboratory **(a)**; soil moisture data measured in the lysimeter **(b)**.

HESSD
9, 3657–3690, 2012

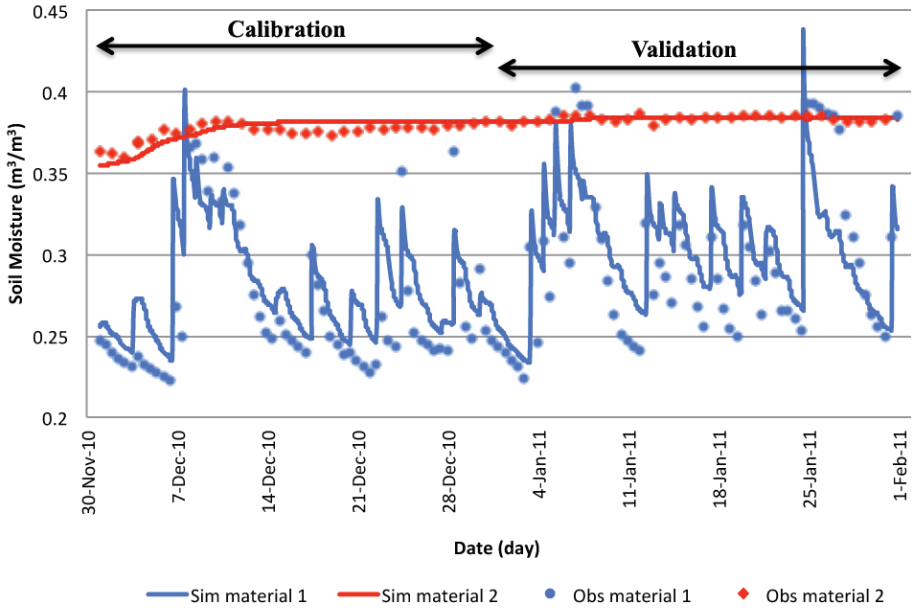

Fig. 4. HYDRUS-1D calibration results (December 2010); HYDRUS-1D validation results (January 2011).

HESSD
9, 3657–3690, 2012

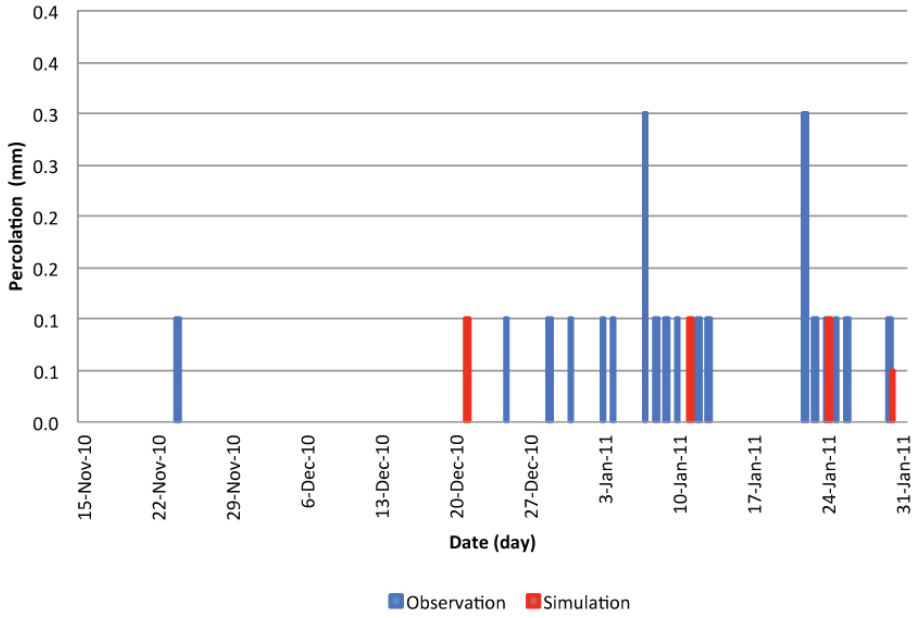

Fig. 5. Percolation observed and simulated by HYDRUS-1D during the experimental period.

HESSD
9, 3657–3690, 2012

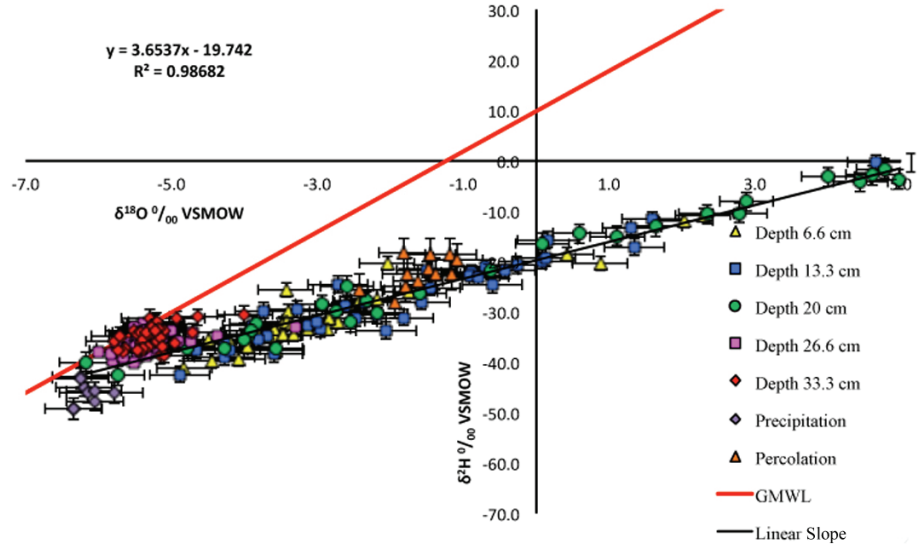

Fig. 6. Isotopes measurement results plotted against GMWL.

HESSD
9, 3657–3690, 2012

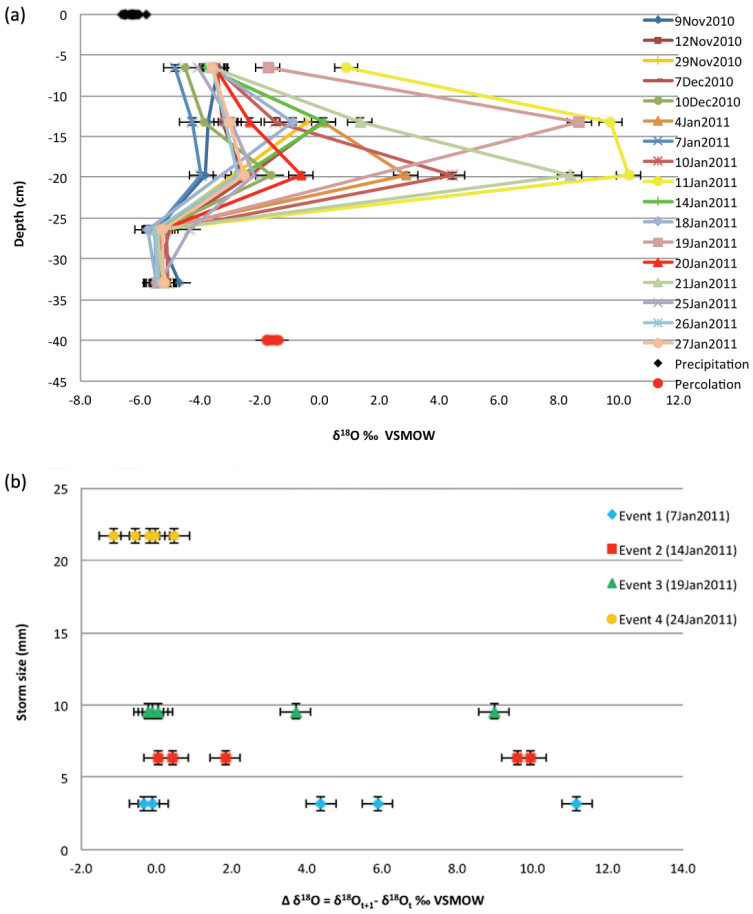

Fig. 7. Isotopes profiles in the lysimeter measured during study period **(a)**; $\Delta^{18}O$ in several precipitation events **(b)**.

HESSD
9, 3657–3690, 2012

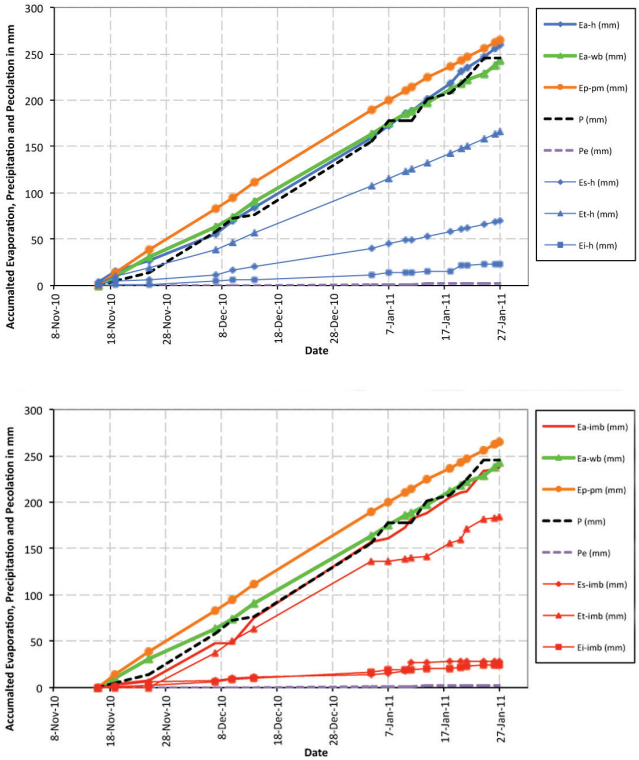

Fig. 8. Comparison of evaporation estimated using four different methods (P for precipitation, P_e percolation, $E_{a\text{-}h}$ evaporation from HYDRUS-1D model, $E_{a\text{-}imb}$ evaporation from isotope mass balance, $E_{a\text{-}wb}$ evaporation from water balance, $E_{p\text{-}pm}$ evaporation from Penman-Monteith, $E_{s\text{-}h}$ soil evaporation from HYDRUS, $E_{t\text{-}h}$ transpiration from HYDRUS, $E_{i\text{-}h}$ interception from HYDRUS, $E_{s\text{-}imb}$ soil evaporation from isotope mass balance, $E_{t\text{-}imb}$ transpiration from isotope mass balance, and $E_{i\text{-}imb}$ interception from isotope mass balance).

HESSD
9, 3657–3690, 2012